

Measurement of the tensor analyzing power A_{yy} in the inelastic scattering of deuterons in the vicinity of excitation of baryonic resonances

V.P. Ladygin^{1,a}, L.S. Azhgirey¹, S.V. Afanasiev¹, V.V. Arkhipov¹, V.K. Bondarev^{1,2}, G. Filipov^{1,3}, A.Yu. Isupov¹, V.I. Ivanov¹, A.A. Kartamyshev⁴, V.A. Kashirin¹, A.N. Khrenov¹, V.I. Kolesnikov¹, V.A. Kuznetsov¹, N.B. Ladygina¹, A.G. Litvinenko¹, S.G. Reznikov¹, P.A. Rukoyatkin¹, A.Yu. Semenov¹, I.A. Semenova¹, G.D. Stoletov¹, V.N. Zhmyrov¹, and L.S. Zolin¹

¹ JINR, 141980, Dubna, Moscow Region, Russia

² St.-Petersburg State University, 198350 St.-Petersburg, Russia

³ Institute of Nuclear Research and Nuclear Energy, 1784 Sofia, Bulgaria

⁴ Russian Scientific Center “Kurchatov Institute”, 123182 Moscow, Russia

Received: 20 April 2000 / Revised version: 10 May 2000

Communicated by M. Garçon

Abstract. The tensor A_{yy} and vector A_y analyzing powers in the inelastic scattering of deuterons with a momentum of 4.5 GeV/c on beryllium at an angle of ~ 80 mr in the vicinity of baryonic resonances excitation have been measured. The A_{yy} data being in good agreement with the previous results obtained at a zero angle demonstrate an approximate t scaling up to ~ -0.9 (GeV/c)². The results of the experiment are compared with the predictions of the multiple-scattering and ω -meson exchange models.

PACS. 24.70.+s Polarization phenomena in reactions – 25.10.+s Nuclear reactions involving few-nucleon systems – 25.70.Ef Resonances

1 Introduction

Hadronic reactions induced by relativistic deuterons have extensively been studied in the last years. In particular, the coherent deuteron interaction (without breakup) with nuclei at high energies has been the subject of such investigations at different laboratories [1–11].

Since the coherent interaction between deuterons and nuclei at relativistic energies involves high momentum transfers, one may expect it to be sensitive to the nuclear structure of the deuteron and, possibly, to the manifestation of non-nucleonic degrees of freedom. In this respect, inelastic scattering of deuterons on nuclei at high momentum transfers can be considered as a complementary method to elastic pd- and ed-scatterings, deuteron breakup reaction, electro- and photodisintegration of the deuteron to investigate the deuteron structure at short distances.

On the other hand, as the deuteron is an isoscalar probe, inelastic scattering of deuterons, $A(d, d')X$, is selective to the isospin of the unobserved system X , which is bound to be equal to the isospin of target A . For instance, this feature was used to search for $\Delta\Delta$ dibaryons with isospin $T = 0$ in the $d(d, d')X$ reaction [6]. Inelastic scattering of deuterons on hydrogen, $H(d, d')X$ is, in

particular, selective to isospin 1/2 and can be used to obtain information on the formation of baryonic resonances $N^*(1440)$, $N^*(1520)$, $N^*(1680)$, and others.

Differential cross-section measurements of deuteron inelastic scattering have been performed at Saclay at 2.95 GeV/c [1, 4] for hydrogen, in Dubna [3, 5, 7] for different targets at deuteron momenta up to 9 GeV/c, and at Fermilab [2] at higher energies for hydrogen. The calculations performed in the framework of multiple-scattering formalism [7] have shown that the differential cross-section of the $H(d, d')X$ reaction can be satisfactorily described by hadron-hadron double scattering. The amplitudes of the elementary processes $NN \rightarrow NN^*$ have been extracted for the $N^*(1440)$, $N^*(1520)$, and $N^*(1680)$ resonances [7].

The experiments have shown a large negative value of T_{20} at a momentum transfer t of ~ -0.3 (GeV/c)². Such a behaviour of the tensor analyzing power has been interpreted in the framework of the ω -meson exchange model [12] due to the longitudinal isoscalar form factor of Roper resonance excitation [13]. The measurements of the tensor and vector analyzing powers A_{yy} and A_y at 9 GeV/c and a 85 mr emission angle of secondary deuterons in the vicinity of an undetected system mass M_X of ~ 2.2 GeV/c² have shown large values which are not explained yet theoretically.

^a e-mail: ladygin@sunhe.jinr.ru

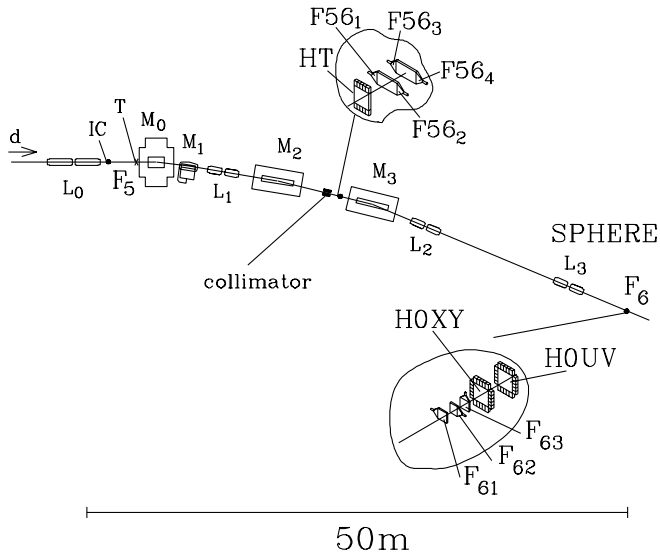


Fig. 1. Layout of the SPHERE setup with beam line VP1. M_i and L_i designate magnets and lenses, respectively; IC is an ionization chamber; T is a target; F_{61} , F_{62} , F_{63} are trigger counters; F_{561-4} are scintillation counters and HT is a scintillation hodoscope for TOF measurements; HOXY and HOUV are beam profile hodoscopes.

In this paper, we report new results on the tensor and vector analyzing powers A_{yy} and A_y in deuteron inelastic scattering on a beryllium target at an incident deuteron momentum of 4.5 GeV/c and a ~ 80 mr secondary emission angle. Details of the experiment are described in sect. 2. A comparison with the existing data and theoretical predictions is made in sect. 3. Conclusions are presented in sect. 4.

2 Experimental method

The experiment has been performed using a polarized deuteron beam at the Dubna Synchrophasotron and the SPHERE setup shown in fig. 1 and described elsewhere [14]. The polarized deuterons were produced by the ion source POLARIS [15]. The sign of beam polarization changed cyclically and spill-by-spill as “0”, “-”, “+”, where “0” means the absence of polarization, “+” and “-” correspond to the sign of p_{zz} with the quantization axis perpendicular to the plane containing the mean beam orbit in the accelerator.

The tensor polarization of the beam was periodically measured during the experiment from the asymmetry of protons in the deuteron breakup reaction on nuclear targets, $d + A \rightarrow p + X$ [16]. This reaction at a zero emission angle and a proton momentum of $p_p \sim \frac{2}{3}p_d$ has a very large tensor analyzing power $T_{20} = -0.82 \pm 0.04$ which is independent of the atomic number of the target ($A > 4$) and the momentum of incident deuterons between 2.5 and 9.0 GeV/c [17]. The tensor polarization averaged over the whole duration of the experiment was $p_{zz}^+ = 0.798 \pm 0.002(\text{stat}) \pm 0.040(\text{sys})$ and $p_{zz}^- =$

$-0.803 \pm 0.002(\text{stat}) \pm 0.040(\text{sys})$ in “+” and “-” beam spin states, respectively.

The stability of beam vector polarization was monitored by measuring the asymmetry of quasi-elastic pp-scattering on a thin CH_2 target placed at focus F_4 of the VP1 beam line ~ 20 m upstream the setup [18]. The values of vector polarization were obtained using the results of asymmetry measurements at a momentum of 4.5 GeV/c per nucleon and a 8° proton scattering angle and the corresponding value of the effective analyzing power of the polarimeter $A(\text{CH}_2)$ taken as 0.146 ± 0.007 [19]. The vector polarization of the beam in different spin states was $p_z^+ = 0.231 \pm 0.014(\text{stat}) \pm 0.012(\text{sys})$ and $p_z^- = 0.242 \pm 0.014(\text{stat}) \pm 0.012(\text{sys})$.

The slowly extracted beam of tensor-polarized 4.5 GeV/c deuterons with an intensity of $5 \cdot 10^8$ particles per beam spill was incident on a beryllium target 20 cm thick positioned at focus F_5 of the VP1 beam line (see fig. 1). The beam intensity was monitored by an ionization chamber placed in front of the target. The beam positions and profiles at certain points of the beam line were monitored by the control system of the accelerator during each spill. The beam size at the target point was $\sigma_x \sim 0.4$ cm and $\sigma_y \sim 0.9$ cm in the horizontal and vertical directions, respectively.

The data were obtained for six momenta of secondary particles between 2.5 and 4.0 GeV/c. The secondary particles emitted at ~ 80 mr from the target were transported to focus F_6 by means of 3 bending magnets (M_0 was switched off) and 3 lenses doublets. The acceptance of the setup was determined via Monte Carlo simulation taking into account the parameters of the incident deuteron beam, nuclear interaction and multiple scattering in the target, in the air, windows and detectors, energy losses of primary and secondary deuterons etc. The momentum and polar angle acceptances were $\Delta p/p \sim \pm 2\%$ and ± 8 mr, respectively.

The coincidences of signals from scintillation counters F_{61} , F_{62} and F_{63} were used as a trigger. Along with the inelastically scattered deuterons, the apparatus detected the protons originating from deuteron fragmentation. The time-of-flight (TOF) information with a base line of ~ 34 m between start counter F_{61} and stop counters $F_{561} - F_{562}$, $F_{563} - F_{564}$ and a scintillation hodoscope HT was used for particle identification in the off-line analysis. The TOF resolution was better than 0.2 ns (1σ). The TOF spectra obtained for all six cases of tuning the magnetic elements are shown in fig. 2. At the higher momentum of detected particles, only deuterons appear in the TOF spectra. However, a relative contribution of protons becomes more pronounced with decreasing momentum. In data processing, useful events were selected as the ones with at least two measured time-of-flight values correlated. This allowed one to rule out the residual background completely. A two-dimensional TOF plot for the detected events with tuning the magnetic elements for 3.6 GeV/c is shown in fig. 3.

The measurement without a target was made for a secondary particle momentum of 4.0 GeV/c. The ratio of

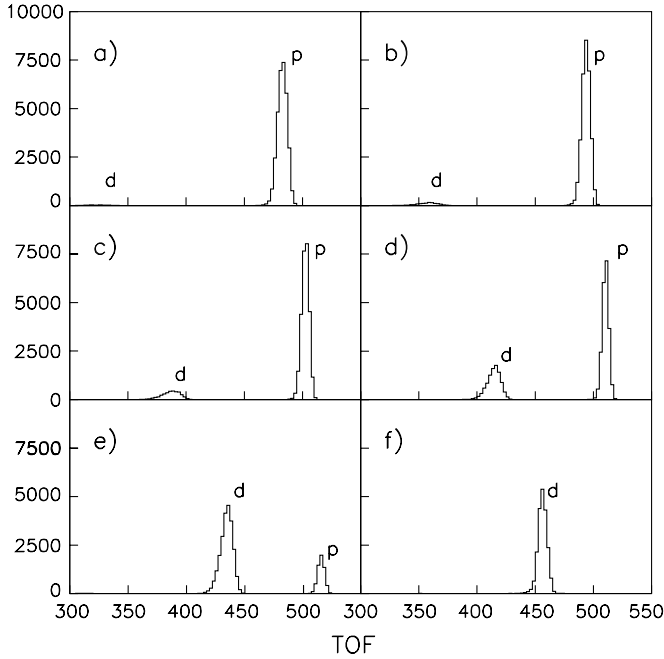


Fig. 2. TOF spectra obtained for different tuning magnetic elements. The panels a), b), c), d), e) and f) correspond to secondary deuteron momenta of 2.5, 2.75, 3.0, 3.3, 3.6, and 4.0 GeV/c, respectively.

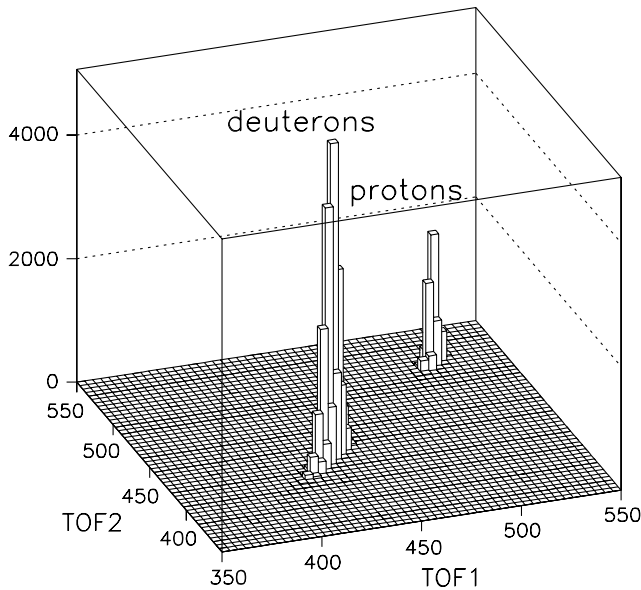


Fig. 3. Two-dimensional plot of two different TOF over a baseline of ~ 34 m at a beam line momentum of ~ 3.6 GeV/c.

the deuteron yields without a target to a 20 cm beryllium target was less than $\sim 1\%$.

The tensor A_{yy} and vector A_y analyzing powers were calculated from the numbers of deuterons n^+ , n^- and n^0 , detected for different states of beam polarization, normalized to the corresponding beam intensities and corrected

for the dead time effect [20]. The calculations were carried out by the expressions

$$A_{yy} = 2 \frac{p_z^- \cdot (n^+ / n^0 - 1) - p_z^+ \cdot (n^- / n^0 - 1)}{p_z^- p_{zz}^+ - p_z^+ p_{zz}^-},$$

$$A_y = -\frac{2}{3} \frac{p_{zz}^- \cdot (n^+ / n^0 - 1) - p_{zz}^+ \cdot (n^- / n^0 - 1)}{p_z^- p_{zz}^+ - p_z^+ p_{zz}^-}. \quad (1)$$

These expressions, taking into account different values of polarization in different beam spin states, are simplified significantly when $p_z^+ = p_z^-$ and $p_{zz}^+ = -p_{zz}^-$.

The data on the tensor A_{yy} and vector A_y analyzing powers in deuteron inelastic scattering obtained in this experiment are given in table 1. The reported error bars are statistical only. The systematic errors are 5% and 8% for A_{yy} and A_y , respectively.

The values of secondary deuteron momentum p , width (FWHM) of momentum acceptance Δp , 4-momentum t , and missing mass M_X given in table 1 are obtained from Monte Carlo simulation. The t -dependence of the differential cross-section of the (d, d')X reaction was taken in the form

$$\frac{d^2\sigma}{dt dM_X^2} \sim e^{-b|t|}, \quad (2)$$

where the slope $b = 18(10)(\text{GeV}/c)^{-2}$ for $M_X \leq 1200$ ($M_X > 1200$) MeV/c² [4]. The averaged momentum of the initial deuteron equals 4.465 GeV/c due to the energy losses in the target.

Since a relatively thick target (36 g/cm²) was used, two-step process, where the deuteron, after its first interaction in the target, elastically scatters on the bound nucleon can contribute. Monte Carlo simulations shows that the contamination of deuterons from this process is no more than 0.5% at a 4.0 GeV/c momentum of secondary particles and decreases with decreasing momenta.

The values of missing mass M_X given in table 1 were calculated under the assumption that the reaction occurs on a target with proton mass. In this case, the 4-momentum transfer t and missing mass M_X are related as follows:

$$M_X^2 = t + m_p^2 + 2m_p Q, \quad (3)$$

where m_p is the proton mass and Q is the energy difference between the incident and scattered deuterons. The dashed area on the kinematic plot given in fig. 4 demonstrates the region of 4-momentum t and missing mass M_X covered by the setup acceptance in the present experiment. The dashed line corresponds to an initial deuteron momentum of 4.5 GeV/c and a zero emission angle [8]. One can see that the same missing mass M_X corresponds to different t under conditions of the previous [8] and present experiments. In this respect, the data obtained at ~ 80 mr provide new information on the t behaviour of the tensor analyzing power A_{yy} .

Table 1. The tensor A_{yy} and vector A_y analyzing powers in the inelastic scattering of 4.5 GeV/c deuterons on beryllium at an angle of ~ 80 mr.

p GeV/c	$\Delta p(\text{FWHM})$ GeV/c	t (GeV/c) ²	M_X GeV/c ²	$A_{yy} \pm dA_{yy}$	$A_y \pm dA_y$
2.577	0.111	-0.917	1.752	-0.178 ± 0.240	0.082 ± 0.272
2.822	0.127	-0.683	1.711	0.070 ± 0.159	-0.072 ± 0.179
3.067	0.139	-0.508	1.647	0.084 ± 0.096	0.053 ± 0.108
3.361	0.149	-0.345	1.549	0.211 ± 0.067	0.015 ± 0.075
3.651	0.165	-0.253	1.418	0.364 ± 0.056	0.155 ± 0.063
4.047	0.189	-0.165	1.196	0.293 ± 0.063	0.098 ± 0.071

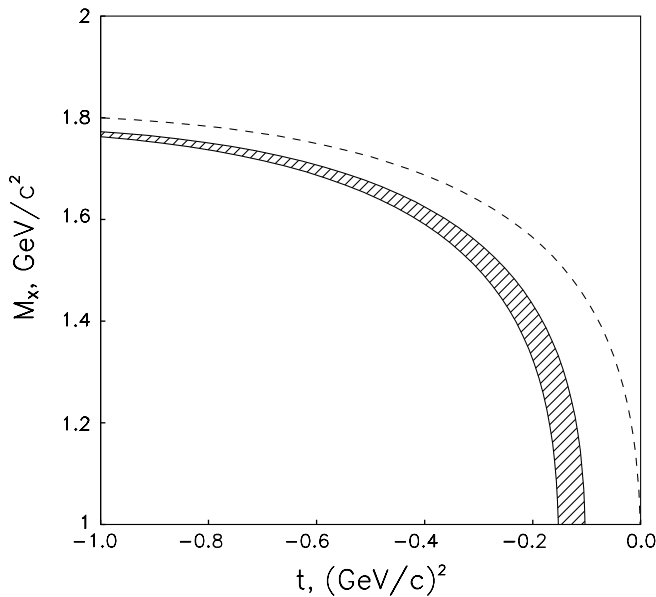


Fig. 4. Kinematic plot of missing mass M_X versus 4-momentum t at an initial deuteron momentum of ~ 4.5 GeV/c. The dashed area demonstrates the region of 4-momentum t and missing mass M_X covered within the acceptance of the present setup, while the dashed line corresponds to the conditions (middle of the acceptance) of the experiment performed at a zero angle [8].

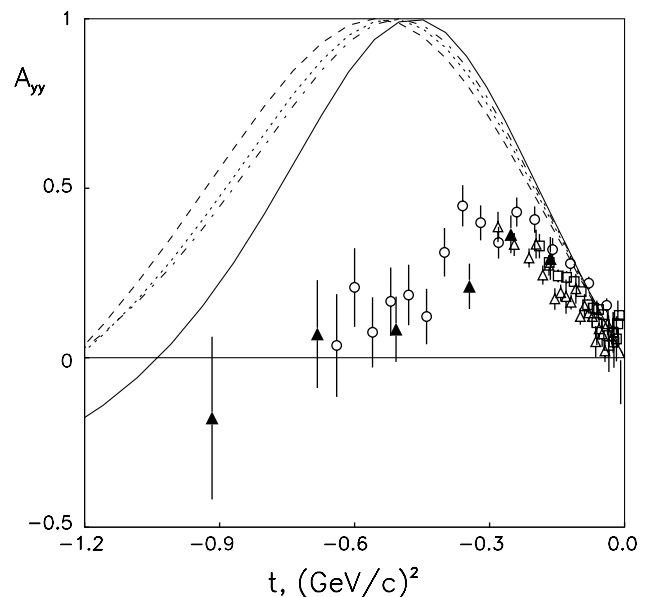


Fig. 5. Tensor analyzing power A_{yy} in deuteron inelastic scattering on beryllium for 4.5 GeV/c at an angle of 80 mr (full triangles) and on hydrogen for 4.5, 5.5 GeV/c [8] and 9 GeV/c [10] at a zero angle plotted as a function of the 4-momentum t and shown by the open triangles, squares and circles, respectively. The solid, dashed, dotted and dash-dotted lines are predictions in the framework of PWIA using DWFs for Paris [21] and Bonn A, B and C [22] potentials, respectively.

3 Results and discussion

Figure 5 presents the data on the tensor analyzing power A_{yy} in the inelastic scattering of 4.5 GeV/c deuterons on beryllium at an angle of 80 mr as a function of 4-momentum t (solid triangles). The A_{yy} has a large positive value of ~ 0.3 over the range of $|t| = 0.2-0.4$ (GeV/c)² and decreases towards zero at larger $|t|$. The data on the tensor analyzing power obtained at a zero emission angle for 4.5, 5.5 GeV/c [8] and 9.0 GeV/c [10] on hydrogen are also given by the open triangles, squares, and circles, respectively (recall that $A_{yy} = -T_{20}/\sqrt{2}$ for these data). One can see a good agreement of the data from our experiment and the previous ones [8,10] in the region where they overlap. The data show an approximative scaling as a function of t with a minor dependence on incident momentum. One can also see, that there is no significant

dependence of A_{yy} on the A -value of the target. This confirms the conclusions drawn earlier in connection with the data at 4.5, 5.5 GeV/c [8] and 9.0 GeV/c [10] obtained at a zero angle. The observed independence of the tensor analyzing power on the atomic number of the target indicates that the rescattering in the target and medium effects (important for the Δ excitation case [23]) are small. Hence, nuclear targets are also appropriate to obtain information on baryonic excitations in deuteron inelastic scattering.

The curves in fig. 5 are the predictions of the A_{yy} behaviour in the framework of the plane-wave impulse approximation (PWIA). Such a mechanism corresponds to the diagram shown in fig. 6a. Within this approach, the tensor analyzing power A_{yy} does not depend on the elementary amplitude $NN \rightarrow NN^*$. It is defined by the charge G_C and quadrupole G_Q form factors of the deuteron as

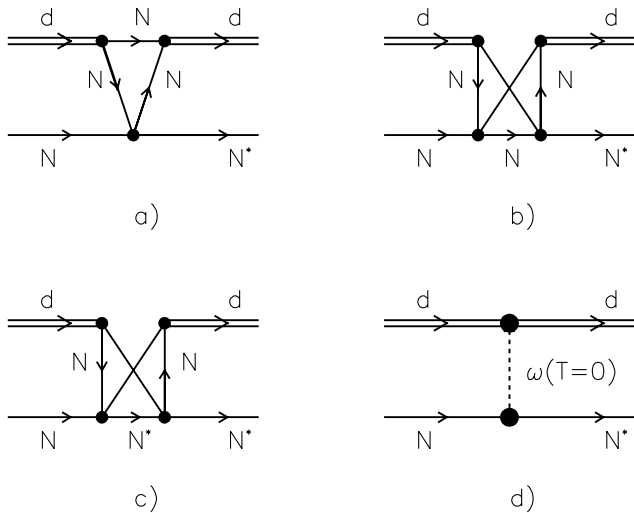


Fig. 6. Diagrams representing mechanisms of baryonic excitation in deuteron-nucleon collisions: a) plane-wave impulse approximation; b) and c) double-collision mechanism; d) ω -meson exchange mechanism.

follows:

$$A_{yy} = \frac{1}{2} \frac{2\sqrt{2}G_C G_Q + G_Q^2}{G_C^2 + G_Q^2}, \quad (4)$$

where

$$G_C(q) = \int_0^\infty (u^2(r) + w^2(r)) j_0(rq/2) dr, \quad (5)$$

$$G_Q(q) = \int_0^\infty 2w(r) \left(u(r) - \frac{w(r)}{2\sqrt{2}} \right) j_2(rq/2) dr. \quad (6)$$

Here $u(r)$ and $w(r)$ are the S and D waves of the deuteron wave function (DWF) in the configuration space; j_0 and j_2 are the Bessel functions of the zero and second order, respectively, and $q^2 = -t$.

The solid line in fig. 5 is calculated with the DWF for Paris potential [21], while the dashed, dotted and dash-dotted lines correspond to the DWFs for Bonn A, B and C potentials [22], respectively. A strong deviation of the present data from the predictions of PWIA, as well as a different behaviour of the tensor analyzing power in the $(d, d')X$ process and in ed - [24,25] and pd - [26] elastic scattering, indicates the sensitivity of A_{yy} to baryonic resonances excitation.

In the framework of the multiple-scattering model, such a deviation may be due to a significant contribution of double-collision interactions corresponding to the diagrams shown in figs. 6b and c. The diagram of fig. 6b describes the situation where the resonance is formed in the second NN collision whereas the resonance in the case of fig. 6c, formed in the first NN interaction, is then elastically scattered on the second nucleon of the deuteron. The calculations have shown that the contribution of the double-scattering terms is significant for $|t|$ greater than ~ 0.4 (GeV/c)² [7]. Therefore, in the framework of

the multiple-scattering model, the behaviour of the tensor analyzing power A_{yy} is defined by the spin structure of the deuteron and the elementary amplitudes of the $NN \rightarrow NN^*$ and $NN^* \rightarrow NN^*$ processes.

The sensitivity of the tensor analyzing power in deuteron inelastic scattering off protons to the excitation of baryonic resonances is pointed out in the framework of the t -channel ω -meson exchange model [12]. The diagram corresponding to this model is shown in fig. 6d. The cross-section and polarization observables can be calculated from the known electromagnetic properties of the deuteron and baryonic resonances N^* through the vector dominance model. The details of the model are given in [12,13], and so we recall main points only briefly in this paper.

In the framework of the ω -meson exchange model, the tensor analyzing power in deuteron inelastic scattering is sensitive to the ratio of the absorption cross-sections of virtual isoscalar photons with longitudinal and transversal polarizations by nucleons $r = \sigma_L/\sigma_T$ [12]:

$$A_{yy} = \frac{V_1^2 + (2V_0V_2 + V_2^2)r}{4V_1^2 + (3V_0^2 + V_2^2 + 2V_0V_2)r}. \quad (7)$$

Here, the structure functions V_0 , V_1 and V_2 are related to the standard electric G_C , magnetic G_M and quadrupole G_Q deuteron form factors [12,13].

In the case of N^* resonance excitation, the ratio r can be written as

$$r_{N^*} = \frac{|A_1^p + A_1^n|^2}{|A_{1/2}^p + A_{1/2}^n|^2 + |A_{3/2}^p + A_{3/2}^n|^2}, \quad (8)$$

where A_1^N is the longitudinal form factor of N^* excitation on proton ($N = p$) or neutron ($N = n$), $A_{1/2}^N$ and $A_{3/2}^N$ are two possible transversal form factors corresponding to the total $\gamma^* + N$ helicity equal to 1/2 and 3/2, respectively. Therefore, in the framework of the ω -meson exchange model in the t -channel [12,13], the tensor analyzing power can be factorized in two parts which are defined, on the one hand, by electromagnetic properties of the deuteron and, on the other hand, by $N \rightarrow N^*$ transition form factors.

The analysis of the t -behaviour of the tensor analyzing power for the $d + p \rightarrow d + X$ process [13] has been performed using the results for the transversal and longitudinal helicity amplitudes from an algebraic collective string model of baryons [27] and taking into account finite width values for the $P_{11}(1440)$, $S_{11}(1535)$, $D_{13}(1520)$, and $S_{11}(1650)$ resonances. However, only the Roper resonance $P_{11}(1440)$ has a nonzero isoscalar longitudinal form factor. The other three considered resonances cannot be excited by isoscalar longitudinal virtual photons, since the isoscalar longitudinal amplitudes of $S_{11}(1535)$ and $D_{13}(1520)$ vanish due to spin-flavor symmetry, while both isoscalar and isovector longitudinal couplings of $S_{11}(1650)$, $D_{15}(1675)$, and $D_{13}(1700)$ vanish identically. Therefore, the t -dependence of the tensor analyzing power in deuteron inelastic scattering is defined in

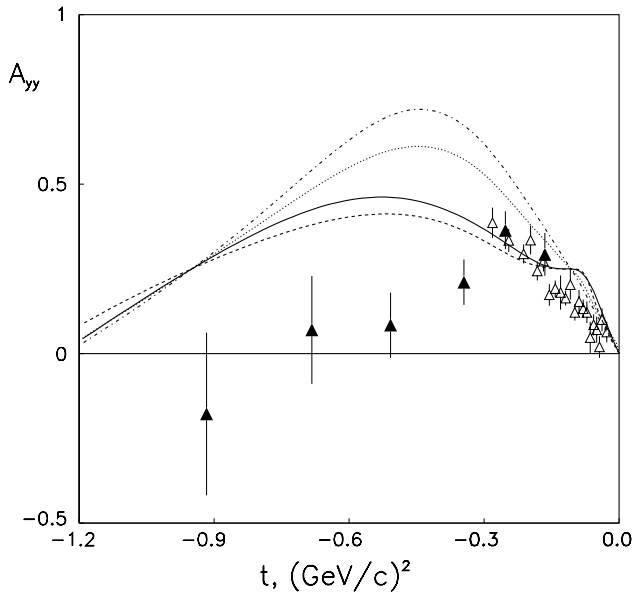


Fig. 7. Tensor analyzing power A_{yy} in the inelastic scattering of 4.5 GeV/c deuterons on beryllium at an angle of ~ 80 mr from the present experiment and on hydrogen at a zero angle [8] plotted *versus* t and shown by the full and open triangles, respectively. The solid and dashed lines are the predictions of the ω -meson exchange model [13] neglecting and taking into account the resonance widths, respectively. The dotted and dash-dotted lines correspond to string stretchability ξ values of 0.5 and 1, respectively.

the framework of the ω -meson exchange model by the contribution of the Roper resonance and the t -dependence of the deuteron form factors [13]. In such an approximation, the tensor analyzing power is a universal function of $|t|$ only, without any dependence on initial deuteron momentum, if the finite values of resonance widths are neglected.

Figure 7 compares the data obtained at 4.5 GeV/c and at ~ 80 mr and zero angles (shown by the full and open triangles, respectively) with the calculations performed in the framework of the ω -meson exchange model [13]. The deuteron form factors from [28], calculated in a relativistic impulse approximation, and standard parameters of the collective string model [27], namely, constituent quark mass $m = 0.366$ GeV, magnetic moment $\mu = 0.127$ GeV $^{-1}$ and the scale parameter of the distribution $a = 0.232$ fm, were used as model inputs. The solid and dashed lines represent results of calculations neglecting and taking into account the finite widths of the resonances, respectively. One can see a reasonable agreement of the calculations with the data up to $|t| \sim 0.3$ (GeV/c) 2 , whereas a serious discrepancy is observed at larger $|t|$. Such a deviation can be related to the contribution from the resonances $F_{15}(1680)$ and $P_{13}(1720)$ neglected in the calculations. Similar to the Roper resonance, they also have nonzero longitudinal isoscalar form factors. Therefore, they can significantly affect the t -dependence of the tensor analyzing power at large $|t|$. On the other hand, the model based on the ω -meson exchange in the t -channel only can be not adequate in this region, and harder processes, for

instance, baryonic excitation in dp-scattering in the one-nucleon exchange approximation [29,30] should be taken into account. Also, exchanges by other mesons (σ , η etc.), as well as the double-scattering mechanism [1,7], may play a significant role at large $|t|$.

In a string model of hadrons, one expects on the basis of QCD that a string elongates (hadrons swell) with increasing excitation energy. The latter can be studied within the collective string model [27] by introducing the stretchability of the string ξ via the ansatz

$$a = a_0 \left(1 + \xi \frac{W - M}{M} \right), \quad (9)$$

where a is the scale parameter of the collective string model with $a_0 = 0.232$ fm, M and W are the nucleon and baryon masses, respectively. The stretchability of the string ξ changes between 0 and 1. The dashed, dotted and dash-dotted lines in fig. 7 are the calculated results in the framework of the ω -meson exchange model [13] with the values of ξ equal to 0, 0.5, and 1, respectively. One can see a strong sensitivity of the tensor analyzing power to ξ . As noted in [13] the introduction of hadrons swelling with $\xi \sim 0.5$ –1 (the last value is consistent with the analysis of the experimental mass spectra, Regge trajectories) gives a better agreement with the experimental data obtained between 3.7 and 9 GeV/c of initial deuteron momentum [8–10]. However, the present data and the ones obtained at 4.5 GeV/c and a zero angle [8] for $|t| \leq 0.3$ (GeV/c) 2 can be described in the framework of the ω -meson exchange model using the value of string stretchability $\xi \sim 0.2$. On the other hand, the mechanisms of Δ -isobar excitation in the projectile and Roper resonance in the target (via σ -meson exchange) [31] should be additionally taken into account in this region. However, in this case the t -dependence of the tensor analyzing power is defined by the interference between the mechanisms considered in [31] and the ω -meson exchange contribution [13] which is sensitive to the value of string stretchability ξ . Therefore, the conclusions concerning the value of ξ cannot be drawn only from the present experimental data in an easy way.

The A_{yy} data from the present experiment (full triangles) along with those obtained at a zero angle and 4.5, 5.5 GeV/c [8] (open triangles and squares, respectively) for four different missing masses M_X of about 1200, 1440, 1550, and 1650 MeV/c 2 *versus* 4-momentum t are shown in fig. 8 a, b, c and d, respectively. The solid and dotted lines are the PWIA calculations using DWFs for Paris [21] and Bonn B [22] potentials, respectively. The points in fig. 8a correspond to the region, where the mechanism of Δ -isobar excitation in the projectile dominates [31] and the tensor analyzing power is mostly defined by the behaviour of the deuteron form factors. The dashed lines in fig. 8 b, c, d are the predictions within the ω -meson exchange model [13] for the excitation of the Roper $P_{11}(1440)$, $D_{13}(1520)$ and $S_{11}(1535)$, and $S_{11}(1650)$ resonances, respectively. As noted above, the t -dependence of the tensor analyzing power is defined by the longitudinal form factor of the Roper resonance only because

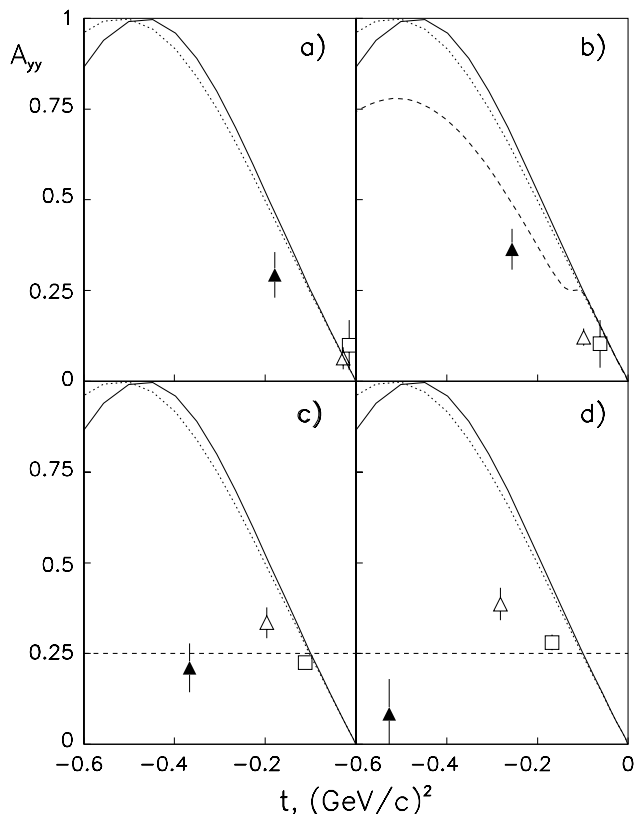


Fig. 8. The A_{yy} data from the present experiment (full triangles) along with the data obtained with 4.5 and 5.5 GeV/c deuterons at a zero angle [8] (open triangles and squares, respectively) at four different missing masses M_X plotted *versus* 4-momentum t : a) at $M_X \sim 1200$ MeV/c², b) at $M_X \sim 1440$ MeV/c², c) at $M_X \sim 1550$ MeV/c², and d) at $M_X \sim 1650$ MeV/c². The solid and dotted lines are the PWIA calculations using DWFs for Paris [21] and Bonn B [22] potentials, respectively. The dashed lines are predictions within the ω -meson exchange model [13].

the longitudinal form factors of the $D_{13}(1520)$, $S_{11}(1535)$, and $S_{11}(1650)$ resonances vanish [13]. In the latter case, the tensor analyzing power A_{yy} is independent of t and equals +0.25. One can see that while the behaviour of A_{yy} is not in contradiction with the ω -meson exchange model prediction [13] in the vicinity of the Roper resonance (fig. 8b) and $M_X \sim 1550$ MeV/c² (fig. 8c), a deviation from a constant value of +0.25 is observed at $M_X \sim 1650$ MeV/c² (fig. 8d). However, as mentioned above, at these missing masses it may be necessary to consider additional contributions from the $F_{15}(1680)$ and $P_{13}(1720)$ resonances which also have nonzero longitudinal isoscalar form factors, and so they can significantly affect the t -dependence of the tensor analyzing power. Note also that a lot of resonances contribute at fixed M_X due to their finite widths since we study the inclusive (d, d')X reaction, while the theoretical predictions in fig. 8 are obtained for separate contributions of the Roper, $S_{11}(1535)$, $D_{13}(1520)$, and $S_{11}(1650)$ resonances. In this respect, exclusive (or semi-exclusive) measurements with the detection of reso-

nance decay products could help to distinguish between the contributions of different baryonic resonances.

The values of the vector analyzing power A_y are small and have large error bars. However, the value of A_y in the vicinity of Roper resonance excitation is 0.155 ± 0.063 , which is not negligible. In the framework of PWIA (see fig. 6a), such a fact can be considered as a significant role of spin-dependent part of the elementary amplitude of the $NN \rightarrow NP_{11}(1440)$ process.

4 Conclusions

We have presented the data on the tensor and vector analyzing powers A_{yy} and A_y in inelastic scattering (d, d')X of 4.5 GeV/c deuterons on beryllium at an angle of ~ 80 mr in the vicinity of the excitations of baryonic masses from 1.2 up to 1.75 GeV/c². This corresponds to the range of 4-momentum $|t|$ between 0.17 and 0.90 (GeV/c)².

The data on A_{yy} demonstrate an approximate t scaling when they are compared with the results obtained at a zero angle [8,10]. It is also seen that A_{yy} does not depend on the A -value of the target. These features of the data indicate that the rescattering, final state interaction, medium effects in nuclei, which depend on kinematics, do not affect the behaviour of the tensor analyzing power significantly.

A strong deviation of A_{yy} in the (d, d')X process from the PWIA prediction, as well as from the behaviour of the tensor analyzing power in ed- [24,25] and pd- [26] elastic scattering, suggests the sensitivity of this observable to the excitation of baryonic resonances via double-collision interactions.

The behaviour of the A_{yy} data obtained in the vicinity of the Roper $P_{11}(1440)$, $S_{11}(1535)$ and $D_{13}(1520)$ resonances is not in contradiction with the predictions of the ω -meson exchange model [13] while this model may require to take into account additional baryonic resonances with nonzero longitudinal form factors at higher excited masses. Such additional mechanisms as double-scattering [1,7], exchanges by other mesons [31] or N^* excitation in the u -channel [29,30] should be also taken into account.

Exclusive polarization experiments with the detection of resonance decay products could significantly advance the understanding of the excitation mechanism of different baryonic resonances and spin properties of their interactions with nucleons.

The authors express their gratitude to A.I. Malakhov, Director of LHE, and V.N. Penev, Vice-Director of LHE, for their permanent help. The authors are grateful to the LHE accelerator staff and POLARIS team for providing good experimental conditions. They thank L.V. Budkin, V.P. Ershov, V.V. Fimushkin, A.S. Nikiforov, Yu.K. Pilipenko, V.G. Pervozchikov, E.V. Ryzhov, A.I. Shirokov, and O.A. Titov for their assistance during the experiment. The authors also thank A.N. Prokofiev and A.A. Zhdanov for lending of scintillation counters for the polarimeter. They are indebted to E. Tomasi-Gustafsson for her permanent help, fruitful discussions and a critical reading of this manuscript.

References

1. J. Banaigs et al., Phys. Lett. B **45**, 535 (1973).
2. Y. Akimov et al., Phys. Rev. Lett. **35**, 763 (1975).
3. L.S. Azhgirei et al., Yad. Fiz. **27**, 1027 (1978) (Sov. J. Nucl. Phys. **27**, 544 (1978)); L.S. Azhgirei et al., Yad. Fiz. **30**, 1578 (1979) (Sov. J. Nucl. Phys. **30**, 818 (1979)).
4. R. Baldini Celio et al., Nucl. Phys. A **379**, 477 (1982).
5. V.G. Ableev et al., Yad. Fiz. **37**, 348 (1983) (Sov. J. Nucl. Phys. **37**, 209 (1983)).
6. M.P. Combet et al., Nucl. Phys. A **431**, 703 (1984).
7. L.S. Azhgirei et al., Yad. Fiz. **48**, 1758 (1988) (Sov. J. Nucl. Phys. **48**, 1058 (1988)).
8. L.S. Azhgirey et al., Phys. Lett. B **361**, 21 (1995).
9. Experiment LNS-E250 (unpublished).
10. L.S. Azhgirey et al., JINR Rapid Commun. **2[88]-98**, 17 (1998).
11. L.S. Azhgirey et al., Yad. Fiz. **62**, 1796 (1999). (Phys. Atom. Nucl. **62**, 1673 (1999)).
12. M.P. Rekaló, E. Tomasi-Gustafsson, Phys. Rev. C **54**, 3125 (1996).
13. E. Tomasi-Gustafsson, M.P. Rekaló, R. Bijker, A. Levitan, F. Iachello, Phys. Rev. C **59**, 1256 (1999).
14. S.V. Afanasiev et al., Phys. Lett. B **434**, 21 (1998).
15. N.G. Anishchenko et al., in *Proceedings of the 5th International Symposium on High Energy Spin Physics, Brookhaven, 1982, AIP Conf. Proc.* **95** (AIP, New York, 1983) p. 445.
16. L.S. Zolin et al., JINR Rapid Commun. **2[88]-98**, 27 (1998).
17. C.F. Perdrisat et al., Phys. Rev. Lett. **59**, 2840 (1987) 2840; V. Punjabi et al., Phys. Rev. C **39**, 608 (1989); V.G. Ableev et al., Pis'ma Zh. Eksp. Teor. Fiz. **47**, 558 (1988) 558. JINR Rapid Commun. **4[43]-90**, 5 (1990) 5; T. Aono et al., Phys. Rev. Lett. **74**, 4997 (1995).
18. L.S. Azhgirey et al., Prib. Tekhn. Exper. **1**, 51 (1997) (Instrum. Exp. Tech. **40**, 43 (1997)).
19. L.S. Azhgirey et al., JINR Rapid Commun. **3[95]-99**, 20 (1999).
20. V.P. Ladygin, Nucl. Instrum. Methods Phys. Res. A **437**, 98 (1999).
21. M. Lacombe et al., Phys. Lett. B **101**, 139 (1981).
22. R. Machleidt et al., Phys. Rep. **149**, 1 (1987).
23. T. Udagawa, P. Oltmanns, F. Osterfeld, S.W. Hong, Phys. Rev. C **49**, 3162 (1994); V. Dmitriev, Nucl. Phys. A **577**, 249c (1994).
24. M. Garçon et al., Phys. Rev. C **49**, 2516 (1994), and references therein.
25. D. Abbott et al., nucl-ex/0001006.
26. V. Ghazikhanian et al., Phys. Rev. C **43**, 1532 (1991).
27. R. Bijker, F. Iachello, A. Levitan, Ann. Phys. (N.Y.) **236**, 69 (1994); Phys. Rev. C **54**, 1935 (1996); Phys. Rev. D **55**, 2865 (1997).
28. P.L. Chung et al., Phys. Rev. C **37**, 2000 (1988).
29. Yu.N. Uzikov, Yad. Fiz. **60**, 1771 (1997) (Phys. Atom. Nucl. **60**, 1616 (1997)).
30. L.S. Azhgirey, N.P. Yudin, JINR preprint P1-99-157, (1999); to be published in Yad. Fiz.
31. S. Hirenzaki, E. Oset, C. Djalali, M. Morlet, Phys. Rev. C **61**, 044605 (2000).